

Fermi golden rule

Transition rate (probability of transition per unit time) :

$$W(t) = W \quad 0 \leq t \leq \tau \quad P_{mn} = \frac{\omega_{mn}}{\tau} = \frac{2\pi}{\hbar} |\langle m|W|n \rangle|^2 \delta(E_m - E_n)$$

Transitions possible only when $E_m = E_n$

$$W(t) = w^\pm e^{\pm i\omega t} \quad 0 \leq t \leq \tau \quad P_{nm} = \frac{\omega_{nm}}{\tau} = \frac{2\pi}{\hbar} |\langle n|w^\pm|m \rangle|^2 \delta(E_n - E_m \pm \hbar\omega)$$

Transitions possible only when $E_m = E_n \pm \hbar\omega$

Electromagnetic disturbance in the form of waves

$$A_{nm} = \frac{\omega_{nm}^3 e^2}{3\pi\epsilon_0 \hbar c^3} |\langle m|\vec{r}|n \rangle|^2 = \frac{4\alpha}{3} \frac{\omega_{nm}^3}{c^2} |\langle m|\vec{r}|n \rangle|^2$$

$$P_{nm} = A_{nm} \delta(E_n - E_m \pm \hbar\omega)$$

2013-02-27 3

Fermi golden rule

Transition rate (probability of transition per unit time) – from the initial state $|i\rangle$ to final $|f\rangle$

$$P_{mn} = \frac{2\pi}{\hbar} |\langle f|W|i \rangle|^2 \rho(E_f)$$

\uparrow \leftarrow
 W - interaction $\rho(E_f)$ - density of final states

Disturbance W is not necessary in the form of electromagnetic wave.

We will be back soon

2013-02-27 4

Interband transitions

Proof:

Carrier's Bloch function

$$\Psi(\vec{r}) = \sum_{n,k} c_{n,k} u_{n,k}(\vec{r}) e^{i\vec{k}\vec{r}}$$

For an electron:

$$\Psi_c(\vec{r}) \approx \sum_k c_{1,k} u_{\Gamma_{6,0}}(\vec{r}) e^{i\vec{k}\vec{r}} = u_{\Gamma_{6,0}}(\vec{r}) F_e(\vec{r})$$

For a hole:

$$\Psi_v(\vec{r}) \approx \sum_{J_z = \pm 3/2, \pm 1/2, k} c_{J_z, k} u_{\Gamma_{8, J_z}}(\vec{r}) e^{i\vec{k}\vec{r}} = \sum_{J_z = \pm 3/2, \pm 1/2, k} u_{\Gamma_{8, J_z}}(\vec{r}) F_h(\vec{r})$$

Dipole optical transitions:

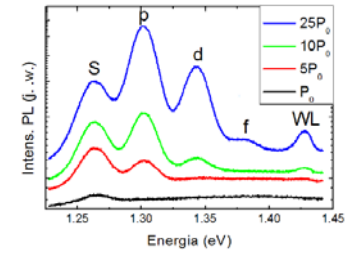
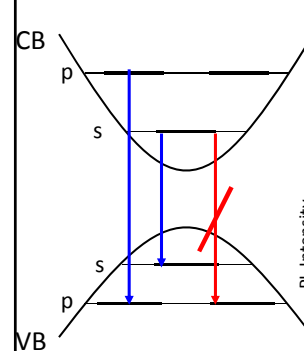
$$\langle \Psi_c(\vec{r}) | \vec{p} | \Psi_v(\vec{r}) \rangle = \langle u_{\Gamma_{6,0}}(\vec{r}) | u_{\Gamma_{8, J_z}}(\vec{r}) \rangle \langle F_e(\vec{r}) | \vec{p} | F_h(\vec{r}) \rangle + \langle u_{\Gamma_{6,0}}(\vec{r}) | \vec{p} | u_{\Gamma_{8, J_z}}(\vec{r}) \rangle \langle F_e(\vec{r}) | F_h(\vec{r}) \rangle$$

$= 0$

2013-02-27

5

Potencjał harmoniczny 2D

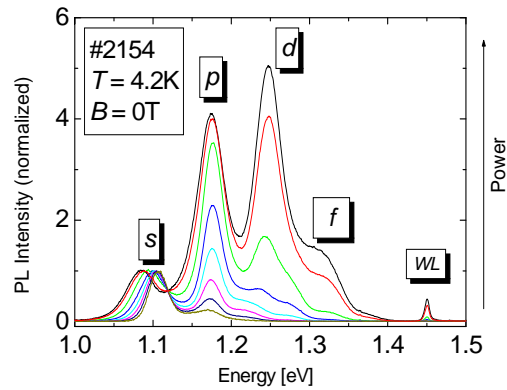


Zależność od mocy pobudzenia widm fotoluminescencji otrzymanych w temperaturze bliskiej temperatury ciekłego helu (ok. 5 K) dla liczego (wielomilionowego) zbioru kropek kwantowych InAs/GaAs.

2013-02-27

6

Potencjał harmoniczny 2D

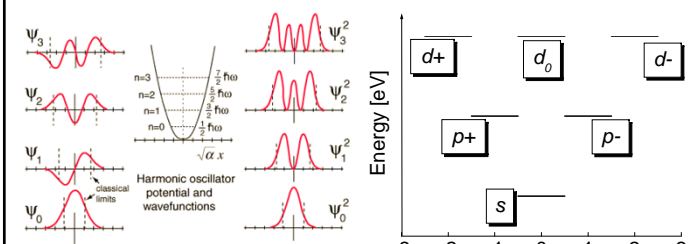


Adam Babiński

2013-02-27

7

Potencjał harmoniczny 2D



$n, m = 0, 1, 2, \dots$
 $L = n - m$ (elektron)

Adam Babiński

2013-02-27

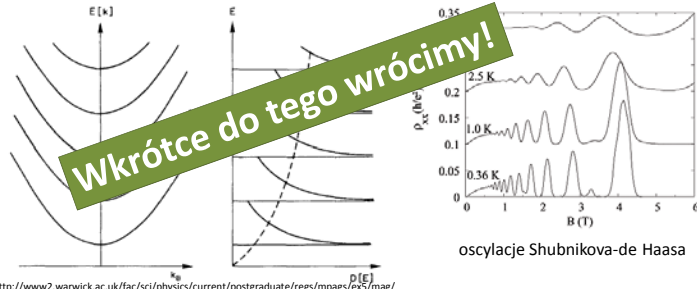
8

Potencjał harmoniczny 2D

$$\left[-\frac{\hbar^2}{2m} \frac{d^2}{dx^2} + \frac{1}{2} m \omega_0^2 x^2 \right] \psi(x) = E \psi(x)$$

$$\omega_0 = \omega_c = \frac{eB}{m^*}$$

Ważny przykład – cząstka w polu magnetycznym. Częstość cyklotronowa ω_c



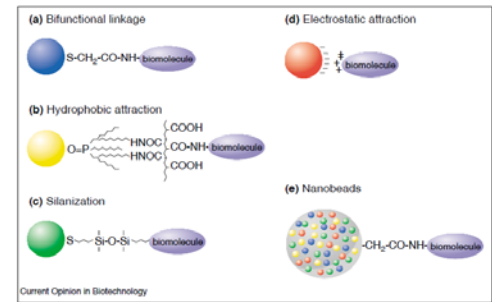
<http://www2.warwick.ac.uk/fac/sci/physics/current/postgraduate/regs/mpags/ocs/mag/>

2013-02-27

9

Sferyczne kropki kwantowe

Schematic illustration of bioconjugation methods. (a) Use of a bifunctional ligand such as mercaptoacetic acid for linking QDs to biomolecules [8**]. (b) TOPO-capped QDs bound to a modified acrylic acid polymer by hydrophobic forces. (c) QD solubilization and bioconjugation using a mercaptosilane compound [7**]. (d) Positively charged biomolecules are linked to negatively charged QDs by electrostatic attraction [9]. (e) Incorporation of QDs in microbeads and nanobeads [20**].



Current Opinion in Biotechnology

Luminescent quantum dots for multiplexed biological detection and imaging
W. Chan et al. Current Opinion in Biotechnology 2002, 13:40–46

2013-02-27

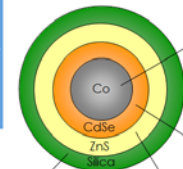
10

Sferyczne kropki kwantowe

Magnetic Quantum Dot
What is MQD?

Justin Galloway

Composite with A Novel Structure for Active Sensing in Living cells



① **Cobalt core : active manipulation**

- + diameter : ~10 nm
- + superparamagnetic NPs
- manipulated or positioned by an external field without aggregation in the absence of an external field

② **CdSe shell : imaging with fluorescence**

- + thickness : 3-5 nm
- + visible fluorescence (~450–700 nm)
- + ability to tune the band gap
- by controlling the thickness, able to tune the emission wavelength, i.e., emission color

③ **Silica shell : bio-compatibility & functionalization with specific targeting group**

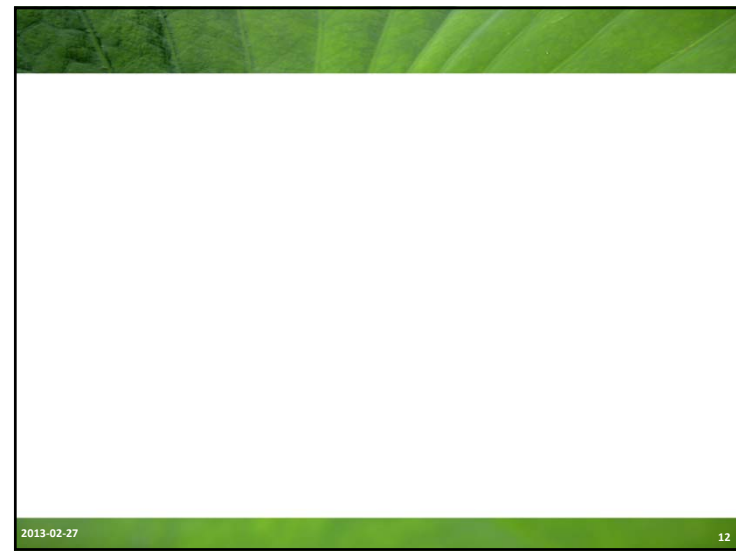
- + thickness : ~10 nm
- + bio-compatible, & non-toxic to live cell functions
- + stable in aqueous environment
- + ability to functionalize its surface with specific targeting group

④ **ZnS shell : electrical passivation**

- + thickness : 1-2 nm
- + having wider band gap (3.83 eV) than CdSe (1.91 eV)
- + enhancement of QY
- CdSe (5-10%) ⇒ CdSe/ZnS (~50%)

2013-02-27

11



2013-02-27

12

Przejścia optyczne

E_f energia końcowa $E_f = E_i + \hbar c Q$ zasada zachowania energii
 E_i energia początkowa $K_f = K_i + Q$ zasada zachowania pędu

Pęd fotonu $\hbar Q = \hbar c Q$. Gdy $\hbar \omega = 1 \text{ eV}$ dostajemy $Q \approx 10^7 \text{ m}^{-1}$. Rozmiar strefy Brillouina to ok. $\frac{\pi}{a} \approx \frac{\pi}{0.5 \text{ nm}} = 10^{10} \text{ m}^{-1}$. Stąd najczęściej $K_f = K_i + Q \approx K_i$

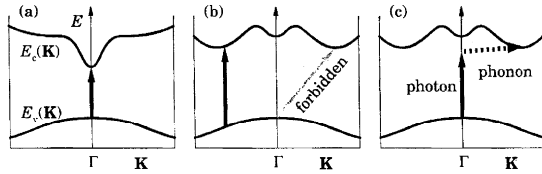


FIGURE 2.2D. Optical absorption across the band gap in different types of semiconductor. (a) Absorption across a direct band gap at Γ . (b) Absorption across an indirect band gap is forbidden but vertical transitions occur for all K . (c) Transition across an indirect band gap with absorption of both a phonon and a photon.

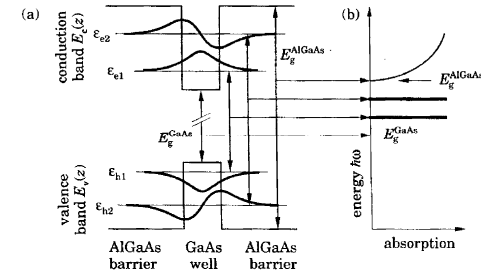
2013-02-27

13

Przejścia optyczne

$$\varepsilon_{e,n_e} = E_c^{GaAs} + \frac{\hbar^2 \pi^2 n_e^2}{2m_0 m_e a^2}$$

$$\varepsilon_{h,n_h} = E_v^{GaAs} - \frac{\hbar^2 \pi^2 n_h^2}{2m_0 m_h a^2}$$



$$\hbar \omega_n = \varepsilon_{e,n_e} - \varepsilon_{h,n_h} = E_g^{GaAs} + \frac{\hbar^2 \pi^2 n^2}{2m_0 a^2} \left(\frac{1}{m_e} + \frac{1}{m_h} \right) = E_g^{GaAs} + \frac{\hbar^2 \pi^2 n^2}{2m_0 m_{eh} a^2}$$

Optyczna masa efektywna: $\frac{1}{m_{eh}} = \frac{1}{m_e} + \frac{1}{m_h}$

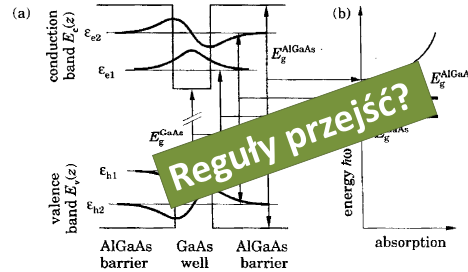
2013-02-27

14

Przejścia optyczne

$$\varepsilon_{e,n_e} = E_c^{GaAs} + \frac{\hbar^2 \pi^2 n_e^2}{2m_0 m_e a^2}$$

$$\varepsilon_{h,n_h} = E_v^{GaAs} - \frac{\hbar^2 \pi^2 n_h^2}{2m_0 m_h a^2}$$



$$\hbar \omega_n = \varepsilon_{e,n_e} - \varepsilon_{h,n_h} = E_g^{GaAs} + \frac{\hbar^2 \pi^2 n^2}{2m_0 a^2} \left(\frac{1}{m_e} + \frac{1}{m_h} \right) = E_g^{GaAs} + \frac{\hbar^2 \pi^2 n^2}{2m_0 m_{eh} a^2}$$

Optyczna masa efektywna: $\frac{1}{m_{eh}} = \frac{1}{m_e} + \frac{1}{m_h}$

2013-02-27

15

Przejścia optyczne

$$\varepsilon_{e,n_e} = E_c^{GaAs} + \frac{\hbar^2 \pi^2 n_e^2}{2m_0 m_e a^2}$$

$$\varepsilon_{h,n_h} = E_v^{GaAs} - \frac{\hbar^2 \pi^2 n_h^2}{2m_0 m_h a^2}$$

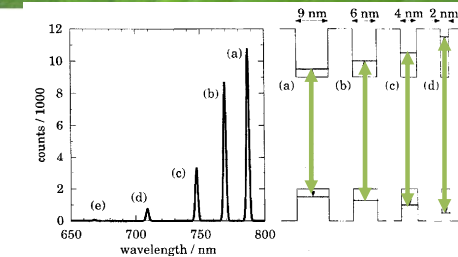


FIGURE 1.4. Photoluminescence as a function of wavelength for a sample with four quantum wells of different widths, whose conduction and valence bands are shown on the right. The barriers between the wells are much thicker than drawn. [Data kindly supplied by Prof. E. L. Hu, University of California at Santa Barbara.]

$$\hbar \omega_n = \varepsilon_{e,n_e} - \varepsilon_{h,n_h} = E_g^{GaAs} + \frac{\hbar^2 \pi^2 n^2}{2m_0 a^2} \left(\frac{1}{m_e} + \frac{1}{m_h} \right) = E_g^{GaAs} + \frac{\hbar^2 \pi^2 n^2}{2m_0 m_{eh} a^2}$$

Optyczna masa efektywna: $\frac{1}{m_{eh}} = \frac{1}{m_e} + \frac{1}{m_h}$

2013-02-27

16

THE ARTICLE

Hidden symmetries in the energy levels of excitonic 'artificial atoms'

M. Bayer*, O. Stern*, P. Hawrylak†, S. Fafard† & A. Forchel*

* Technische Physik, Universität Würzburg, Am Hubland, D-97074 Würzburg, Germany

† Institute for Microstructural Science, National Research Council of Canada, Ottawa, K1A 0R6, Canada

NATURE | VOL 405 | 22 JUNE 2000 | www.nature.com

THE ARTICLE

- jakie są to kropki, jakich energii luminescencji się spodziewamy?
- jaką metodą otrzymano te kropki? Jak je przygotowano do eksperymentu i dlaczego było to konieczne?
- dlaczego pomiary są w temperaturach helowych? Jakie są skale energii?
- w jaki sposób opisane są procesy zachodzące w kropkach? Czy umiesz przeczytać hamiltonian „słowami”?
- jakiej energii używamy do pobudzenia?
- co się zmienia z mocą pobudzenia?
- widmo emisyjne opisane jest „złotą regułą Fermiego” – o co chodzi?
- dlaczego niektóre linie „gasną”, a inne „się pojawiają” jak świecimy coraz mocniej?
- dlaczego jest mowa o „sztucznych atomach”? Jaki jest czas życia (rozpadu) takiego atomu? Jak wygląda „szereg promieniotwórczy” sztucznych atomów?
- o jakie ukryte symetrie chodzi w artykule?
- do czego można by wykorzystać obserwowane efekty?

THE ARTICLE

ARTIFICIAL ATOMS

The charge and energy of a sufficiently small particle of metal or semiconductor are quantized just like those of an atom. The current through such a quantum dot or one-electron transistor reveals atom-like features in a spectacular way.

Marc A. Kastner

M A Kastner, *Phys. Today*, **46**, 24 (1993)

REVIEW ARTICLE

Electrons in artificial atoms

R. C. Ashoori

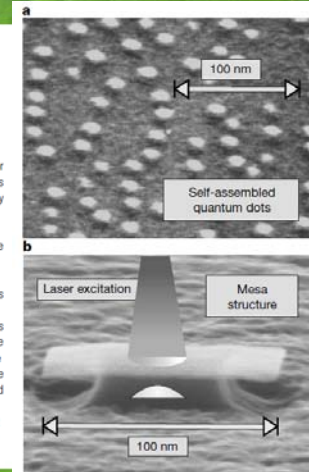
Progress in semiconductor technology has enabled the fabrication of structures so small that they can contain just one mobile electron. By varying controllably the number of electrons in these 'artificial atoms' and measuring the energy required to add successive electrons, one can conduct atomic physics experiments in a regime that is inaccessible to experiments on real atoms.

R C Ashoori, *Nature*, **379**, 413 (1996)

THE ARTICLE

NATURE | VOL 405 | 22 JUNE 2000 | www.nature.com

Figure 1 Scanning electron micrographs illustrating the experimental technique used for studying single self-assembled quantum dots. **a**, Scanning electron micrograph of a GaAs semiconductor layer on which $\text{In}_{0.47}\text{Ga}_{0.53}\text{As}$ self-assembled quantum dots with a density of about 10^{10} cm^{-2} have been grown by molecular beam epitaxy. To permit their microscopic observation these dots—unlike those used for spectroscopy—have not been covered by a GaAs cap layer. To a good approximation, all quantum dots have the same shape exhibiting rotational symmetry. However, their size varies by a few nanometres around an average diameter of 15 nm. This inhomogeneity results in a considerable broadening of the emission lines in spectroscopic studies. **b**, To avoid this broadening we have studied the emission of a single quantum dot. Lithographic techniques were used to fabricate small mesa structures on samples capped by a GaAs layer. The lateral mesa size was reduced to such an extent (<100 nm) that only a single dot is contained in it. These mesa structures have been studied by photoluminescence spectroscopy at low temperature. A laser beam (shown schematically as a truncated cone above the mesa) injects a controlled number of electrons and holes into the dot indicated by the lens shape, and the emission spectrum of this complex is recorded. To reduce sample heating under optical excitation, the structures are held in superfluid helium at about 1.2 K. After dispersion by a monochromator, the emission is detected by a CCD (charge-coupled device) camera.



Harmonic potential 2D

$E_n^x = \hbar\omega_0 \left(n_x + \frac{1}{2} \right)$ in x direction and the same in y

$E_n^y = \hbar\omega_0 \left(n_y + \frac{1}{2} \right)$

$$E_n = E_n^x + E_n^y = \hbar\omega_0(N + 1)$$

Degeneracy? $N = n_x + n_y$

$$g_N = N + 1$$

N	(n_x, n_y)
0	(0,0)
1	(1,0) (0,1)
2	(2,0) (1,1) (0,2)
3	(3,0) (2,1) (1,2) (0,3)

2D disk shaped dot

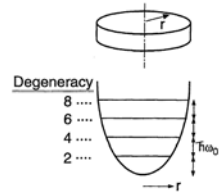


Fig. 5. Schematic model for the vertical dot with a harmonic lateral potential. The single-particle states are laterally confined into discrete equidistant OD levels whose degeneracies are 2, 4, 6, 8, ... including spin degeneracy from the lowest level.

Jpn. J. Appl. Phys., Vol. 36 (1997) pp. 3917-3923 Part 1, No. 6B, June 1997

Harmonic potential 3D

$E_n^x = \hbar\omega_0 \left(n_x + \frac{1}{2} \right)$ in x, y, z

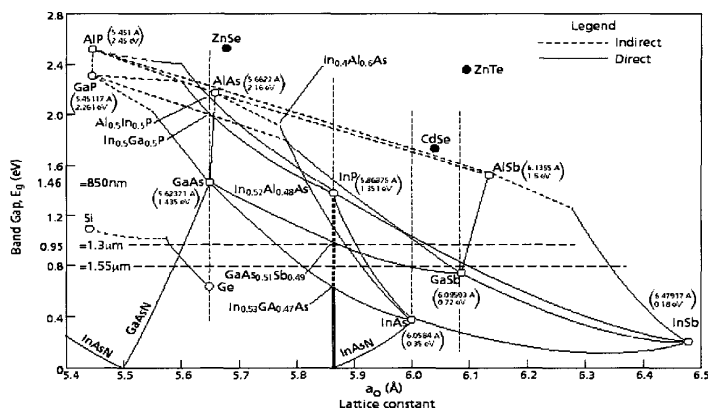
$$E_n = E_n^x + E_n^y + E_n^z = \hbar\omega_0 \left(N + \frac{3}{2} \right)$$

Degeneracy? $N = n_x + n_y + n_z$

$$g_N = \frac{(N+1)(N+2)}{2}$$

N	(n_x, n_y, n_z)
0	(0,0,0)
1	(1,0,0) (0,1,0) (0,0,1)
2	(2,0,0) (0,2,0) (0,0,2) (1,1,0) (1,0,1) (0,1,1)
3	3x(3,0,0) 1x(1,1,1) 6x(2,0,1)

Semiconductor heterostructures



Investigation of high antimony-content gallium arsenide nitride-gallium arsenide antimonide heterostructures for long wavelength application

THE ARTICLE

NATURE | VOL 405 | 22 JUNE 2000 | www.nature.com

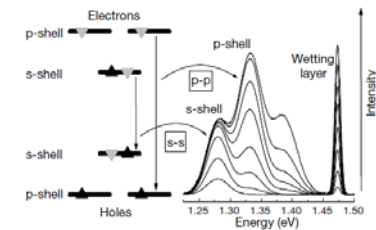


Figure 2 State filling spectroscopy on quantum dots. On the left is a scheme of the dot energy levels, their occupation by carriers and the radiative transitions. Spin orientations of electrons and holes; grey triangles, spin-down; black triangles, spin-up. On the right are typical emission spectra resulting from these transitions for an ensemble of $In_{0.67}Ga_{0.33}As$ quantum dots; these spectra were recorded at different excitation powers (an Ar-ion laser was used).

THE ARTICLE

NATURE | VOL 405 | 22 JUNE 2000 | www.nature.com

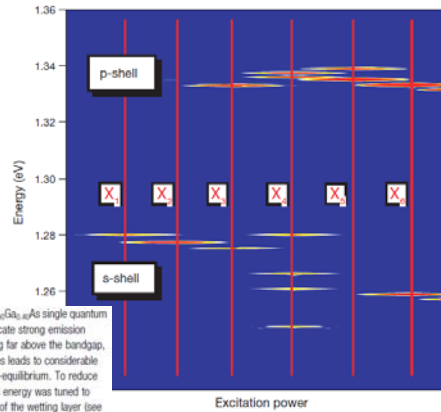
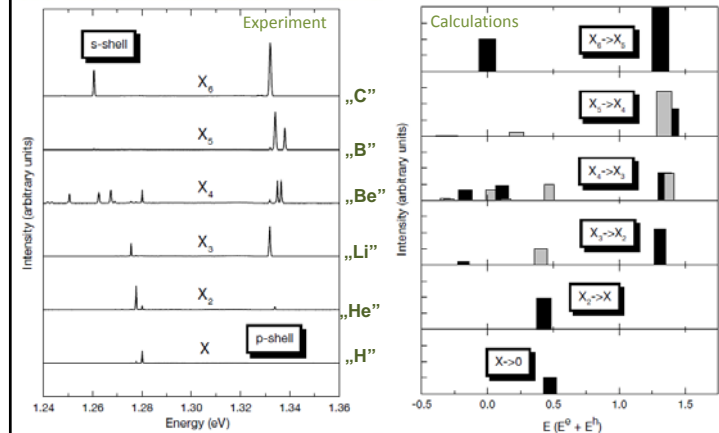


Figure 3 Contour plot of the variation of the emission of an InGaAs single quantum dot with excitation power and with energy. Bright regions indicate strong emission intensities, blue regions low intensities. When optically exciting far above the bandgap, carrier relaxation involving multiple phonon emission processes leads to considerable sample heating, which causes the system to be in strong non-equilibrium. To reduce heating, a Ti-sapphire laser was used as excitation source. Its energy was tuned to $E = 1.470$ eV, corresponding to emission close to the bottom of the wetting layer (see Fig. 2). The excitation power P_{ex} was varied between 50 nW and 5 mW.

2013-02-27

25

THE ARTICLE



2013-02-27

26

THE ARTICLE

NATURE | VOL 405 | 22 JUNE 2000 | www.nature.com

$$H = \sum_i E_i^e c_i^\dagger c_i + \sum_i E_i^h d_i^\dagger d_i - \sum_{ij} (ij|V_{eh}|k\ell) c_i^\dagger d_j^\dagger d_k c_\ell + \frac{1}{2} \sum_{ijkl} (ij|V_{ee}|k\ell) c_i^\dagger c_j^\dagger c_k c_\ell + \frac{1}{2} \sum_{ijkl} (ij|V_{hh}|k\ell) d_i^\dagger d_j^\dagger d_k d_\ell$$

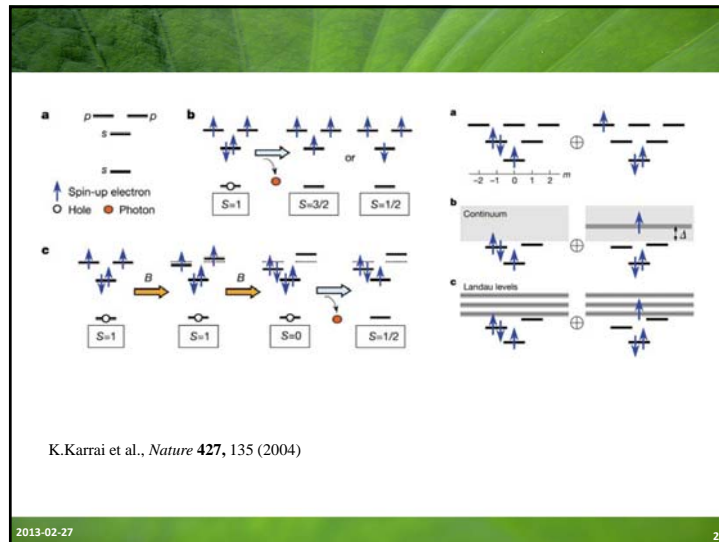
where c_i^\dagger and d_i^\dagger (c_i and d_i) are the creation (annihilation) operators for electrons and holes. $E_i^{e/h}$ are the electron/hole single particle energies and V_{mn} , $m, n = e, h$ are the interparticle Coulomb interactions.

The interband optical processes are described by the polarization operator $P^\dagger = \sum_i c_i^\dagger d_i^\dagger$, where P^\dagger annihilates a photon and creates an electron-hole pair. The main question arises when populating

$$L_N(\omega) = \sum_j \langle (N-1, j|P^-|i, N) \rangle^2 \delta(E_N - E_{N-1} - \hbar\omega)$$

2013-02-27

27



K. Karrai et al., *Nature* 427, 135 (2004)

2013-02-27

28